

Electronic Supplementary Information

Structural regulation of NHC-protected Copper(I) clusters through substituent effect for photoluminescence enhancement

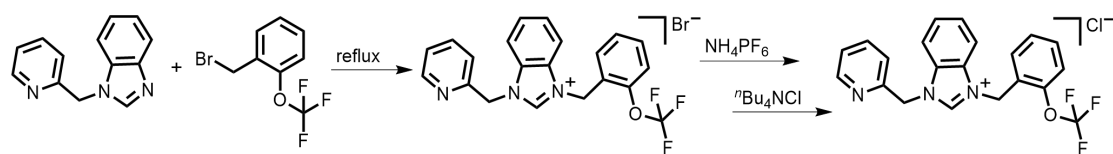
Yan-Yan Yang,^a Rui-Chen Hao,^a Qing-Qing Wu,^b Peng Luo,^{*a,b} Jun Xu,^{*a} Xi-Yan Dong^{*a,b}
and Chuan-Xiang Zhang^a

^a College of Chemistry and Chemical Engineering, Henan Polytechnic University,
Jiaozuo 454003, China

^b College of Chemistry, Zhengzhou University, Zhengzhou 450001, China

Synthesis of benzimidazole precursors

Synthesis of 1-(2-trifluoromethoxybenzyl)-3-picolyl-benzimidazolium chloride ($\text{NHC}^{\text{PyOF}} \cdot \text{HCl}$)



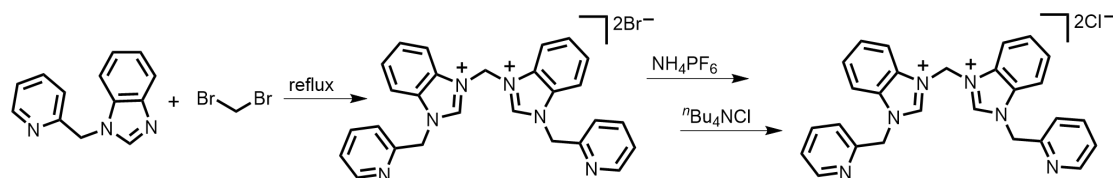
Scheme S1. Synthetic procedure of $\text{NHC}^{\text{PyOF}} \cdot \text{HCl}$.

$\text{NHC}^{\text{PyOF}} \cdot \text{HBr}$ was synthesized based on the modified methods in previous literature.^{S1} N-picolylbenzimidazole (2.1 g, 10 mmol) and 2-(trifluoromethoxy)benzyl bromide (7.17 g, 30 mmol) were mixed together in 100 mL of toluene. The mixture was refluxed overnight, then the white solid was isolated and washed with several portions of ethyl acetate to get $\text{NHC}^{\text{PyOF}} \cdot \text{HBr}$ (3.75 g, 8 mmol). Yield 84%.

$\text{NHC}^{\text{PyOF}} \cdot \text{HPF}_6$: In a flask, $\text{NHC}^{\text{PyOF}} \cdot \text{HBr}$ (448 mg, 1 mmol) was dissolved in 3 mL methanol, and NH_4PF_6 (489 mg, 3 mmol) aqueous solution was added dropwise. The precipitate was formed during 12 h. The reaction mixture was filtered, washed thoroughly with water/methanol, and dried *in vacuo*, which was used for the next reaction without further purification.

$\text{NHC}^{\text{PyOF}} \cdot \text{HCl}$: In a flask, the above $\text{NHC}^{\text{PyOF}} \cdot \text{HPF}_6$ was dissolved in 3 mL acetonitrile, and $n\text{Bu}_4\text{NCl}$ (834 mg, 3 mmol) in acetonitrile was added dropwise. The precipitate was formed during 12 h. The reaction mixture was filtered, washed thoroughly with acetonitrile, and dried *in vacuo*. The compound was further purified by recrystallization from methanol/diethyl ether to get off-white solid as $\text{NHC}^{\text{PyOF}} \cdot \text{HCl}$ (330 mg, 0.82 mmol). Yield 82% (two-step overall yield). ^1H NMR ($\text{DMSO}-d_6$): 9.97 (s, 1H), 8.50-8.49 (d, 1H), 8.02-8.01 (d, 1H), 7.93-7.90 (m, 2H), 7.79-7.66 (m, 6H), 7.39-7.29 (m, 2H), 6.05-5.99 (d, 4H).

Synthesis of bis-(2-picolyl-benzimidazolyl)methane chloride ($\text{bisNHC}^{\text{Me}} \cdot (\text{HCl})_2$)



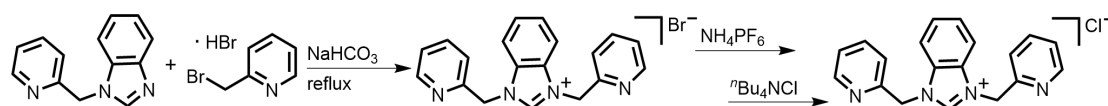
Scheme S2. Synthetic procedure of $\text{bisNHC}^{\text{Me}} \cdot (\text{HCl})_2$.

$\text{bisNHC}^{\text{Me}} \cdot (\text{HBr})_2$ was synthesized based on the modified methods in previous literature.^{S1} N-picolylbenzimidazole (2.1 g, 10 mmol) and dibromomethane (0.87 g, 5 mmol) were mixed together in 100 mL of toluene. The mixture was refluxed overnight, then the white solid was isolated and washed with several portions of ethyl acetate get $\text{bisNHC}^{\text{Me}} \cdot (\text{HBr})_2$ (3.85 g, 0.65 mmol). Yield 65%.

bisNHC^{Me}•(HPF₆)₂: In a flask, **bisNHC^{Me}•(HBr)₂** (591 mg, 1 mmol) was dissolved in 3 mL methanol, and NH₄PF₆ (489 mg, 3 mmol) aqueous solution was added dropwise. The precipitate was formed during 12 h. The reaction mixture was filtered, washed thoroughly with water/methanol, and dried *in vacuo*, which was used for the next reaction without further purification.

bisNHC^{Me}•(HCl)₂: In a flask, the above **bisNHC^{Me}•(HPF₆)₂** was dissolved in 3 mL acetonitrile, and ⁿBu₄NCl (834 mg, 3 mmol) in acetonitrile was added dropwise. The precipitate was formed during 12 h. The reaction mixture was filtered, washed thoroughly with acetonitrile, and dried *in vacuo*. The compound was further purified by recrystallization from methanol/diethyl ether to get off-white solid as **bisNHC^{Me}•(HCl)₂** (413 mg, 0.82 mmol). Yield 82% (two-step overall yield). ¹H NMR (DMSO-*d*₆): 10.63 (s, 2H), 8.46 (d, 2H), 8.40-8.38 (d, 2H), 8.05-7.39 (m, 14H), 6.04 (s, 4H).

Synthesis of 1, 3-bis-picolyl-benzimidazolium chloride (NHC^{Py2}•HCl)



Scheme 3. Synthetic procedure of NHC^{Py2}•HCl.

NHC^{Py2}•HBr was synthesized based on the modified methods in previous literature.^{S2} In a Schlenk flask, N-picolylbenzimidazole (2.1 g, 10 mmol) and 2-(bromomethyl)pyridine hydrobromide (278 mg, 1.1 mmol) were dissolved in 20 mL CH₃CN under an argon atmosphere. The mixture was stirred at room temperature for 10 min, and then NaHCO₃ (168 mg, 2 mmol) was added in one portion. The reaction mixture was refluxed for 48 h, and then cooled to room temperature. The solvent was removed *in vacuo* and then DCM was added to get brown suspension, which was filtered to collect the liquid part. The solvent was concentrated *in vacuo*, followed by recrystallization from CH₂Cl₂/EtOAc to afford a light brown solid as **NHC^{Py2}•HBr** (362 mg, 0.95 mmol). Yield 95%.

NHC^{Py2}•HPF₆: In a flask, **NHC^{Py2}•HBr** (381 mg, 1 mmol) was dissolved in 3 mL methanol, and NH₄PF₆ (489 mg, 3 mmol) aqueous solution was added dropwise. The precipitate was formed during 12 h. The reaction mixture was filtered, washed thoroughly with water/methanol, and dried *in vacuo*, which was used for the next reaction without further purification.

NHC^{Py2}•HCl: In a flask, the above **NHC^{Py2}•HPF₆** was dissolved in 3 mL acetonitrile, and ⁿBu₄NCl (834 mg, 3 mmol) in acetonitrile was added dropwise. The precipitate was formed during 12 h. The reaction mixture was filtered, washed thoroughly with acetonitrile, and dried *in vacuo*. The compound was further purified by recrystallization from methanol/diethyl ether to get off-white solid as **NHC^{Py2}•HCl** (275 mg, 0.82 mmol). Yield 82% (two-step overall yield). ¹H NMR (DMSO-*d*₆): 10.63 (s, 2H), 8.46 (d, 2H), 8.40-8.38 (d, 2H), 8.05-7.39 (m, 14H), 6.04 (s, 4H).

Measurements

^1H NMR spectra were recorded on a Bruker DRX spectrometer operating at 600 MHz. Electrospray ionization mass spectrometry (ESI-MS) measurements were recorded on a SCIEX X500R QTOF spectrometer. Elemental analysis measurements (H, C, and N) were conducted with an Elementar UNICUBE elemental analyzer under CHNS mode. Powder X-ray diffraction (PXRD) was performed on a Rigaku D/Max-2500PC X-ray diffractometer with a Cu sealed tub ($\lambda = 1.54178 \text{ \AA}$). UV-Vis absorption spectra were recorded using a Hitachi UH4150 UV-visible spectrophotometer. Emission spectra were recorded with an Edinburgh FLS 980 fluorescence spectrometer. Luminescence lifetime was measured on an Edinburgh FLS 1000 fluorescence spectrometer equipped with a 355 nm laser operating in time-correlated single-photon counting mode (TCSPC) with a resolution time of 340 μs . The photoluminescence quantum efficiency was measured in the range of 400-950 nm using an integrating sphere on a HAMAMATSU Quantaaurus-QY spectrofluorometer. Fourier transform infrared (FT-IR, Thermo., NEXUS FT-IR) spectra were recorded as KBr pellets at a resolution of 4 cm^{-1} to observe the functional groups.

Single-crystal X-ray diffraction analyses

Single-crystal X-ray diffraction (SCXRD) measurements of clusters were performed on a Rigaku XtaLAB Pro diffractometer using Cu $K\alpha$ radiation ($\lambda = 1.54184 \text{ \AA}$) and Mo $K\alpha$ ($\lambda = 0.71073$). Data collection and reduction were performed using the program *CrysAlisPro*.⁵³ All the structures were solved with direct methods (*SHELXS*) and refined by full-matrix least squares on F^2 using *OLEX2*, which utilizes the *SHELXL-2015* module.⁵⁴⁻⁵⁶ All atoms were refined anisotropically, and hydrogen atoms were placed in calculated positions with idealized geometries and assigned fixed isotropic displacement parameters. Detailed information about the X-ray crystal data, intensity collection procedure, refinement results and selected bond lengths for all cluster compounds were summarized in the Supporting Information Table S4-S9.

Density Functional Theory (DFT) calculations

The Density Functional Theory (DFT) and Time-Dependent Density Functional Theory (TDDFT) calculations were performed with Gaussian 16 under the Perdew–Burke–Ernzerhof (PBE)

exchange-correlation functional using def2SVP core pseudopotential for all atoms.⁵⁷⁻⁵⁸ The single-crystal structure was chosen as the initial guess for ground-state optimization, and all reported stationary points were verified as true minima by the absence of negative eigenvalues in the vibrational frequency analysis. The UV–Vis and IGMH analysis were conducted by Multiwfn program.⁵⁹

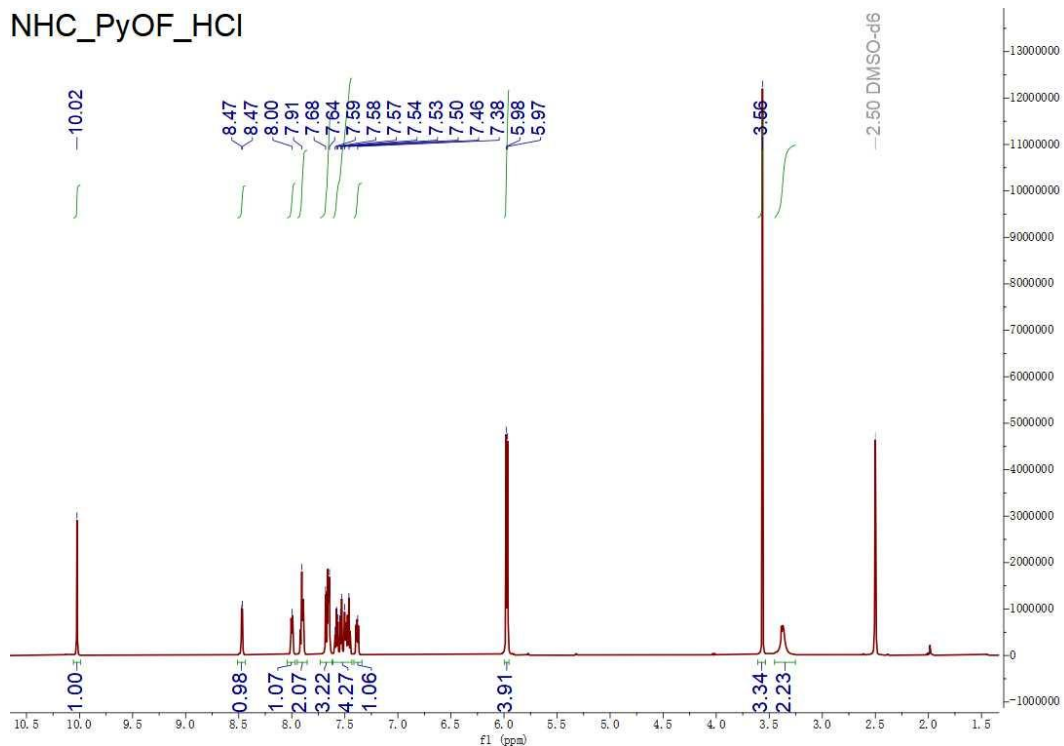


Figure S1. ^1H NMR of $\text{NHC}^{\text{PyOF}}\bullet\text{HCl}$ in $\text{DMSO-}d_6$.

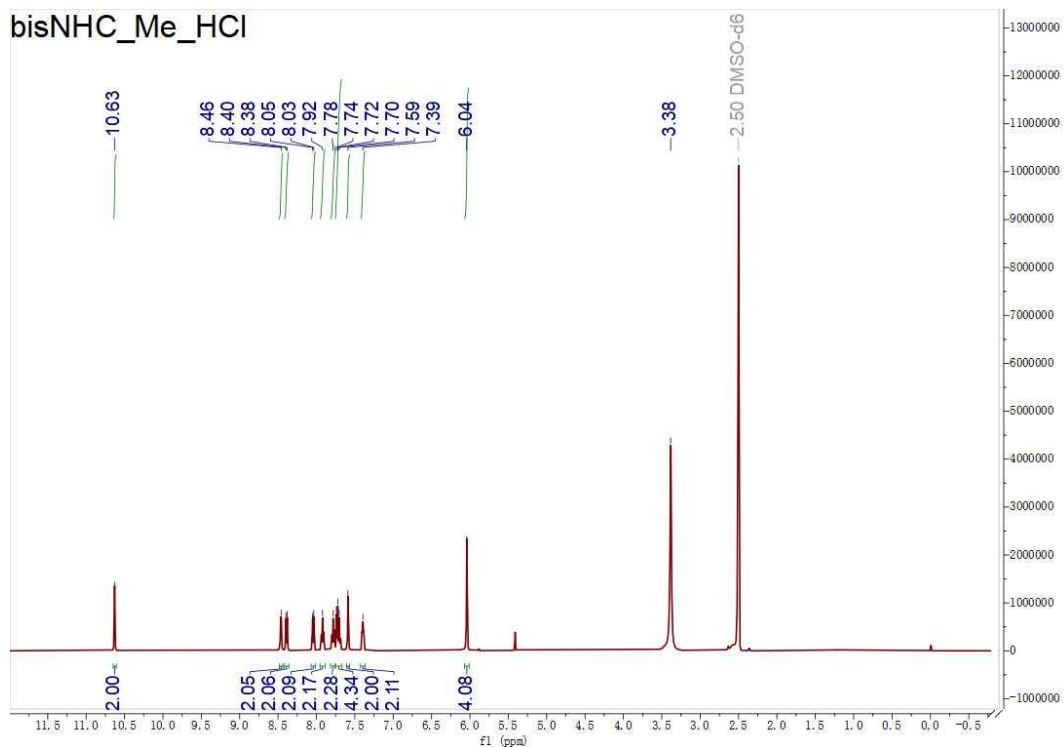


Figure S2. ^1H NMR of $\text{bisNHC}^{\text{Me}}\bullet(\text{HCl})_2$ in $\text{DMSO-}d_6$.

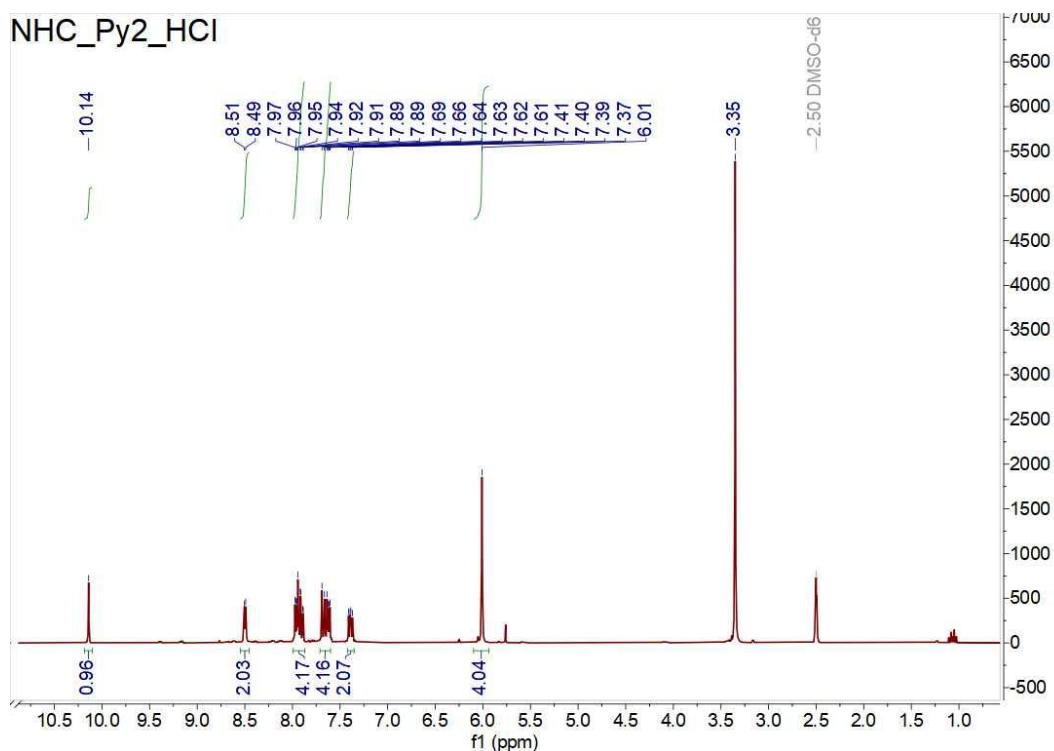


Figure S3. ^1H NMR of $\text{NHC}^{\text{Py}2}\cdot\text{HCl}$ in $\text{DMSO-}d_6$.

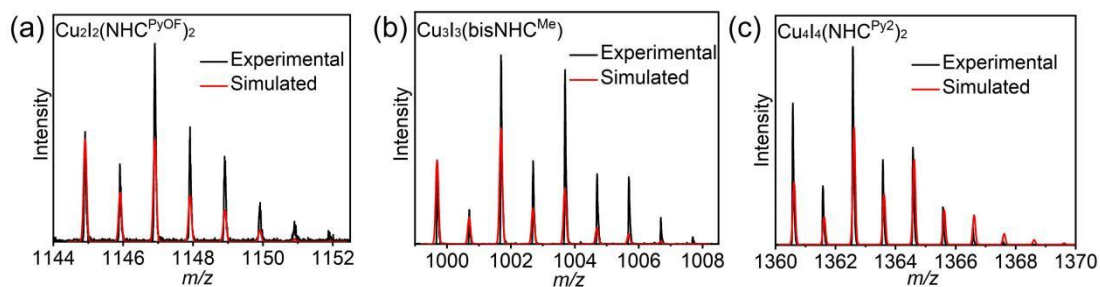


Figure S4. ESI-MS spectra for (a) $\text{Cu}_2\text{I}_2(\text{NHC}^{\text{PyOF}})_2$; (b) $\text{Cu}_3\text{I}_3(\text{bisNHC}^{\text{Me}})$ and (c) $\text{Cu}_4\text{I}_4(\text{NHC}^{\text{Py}2})_2$ clusters. $[\text{Cu}_2\text{I}_2\text{C}_{42}\text{H}_{33}\text{N}_6\text{O}_2\text{F}_6]^+$: $m/z = 1146.8427$ (calcd. 1146.8587); $[\text{Cu}_3\text{I}_3\text{C}_{27}\text{H}_{23}\text{N}_6]^+$: $m/z = 1001.6591$ (calcd. 1001.6547); $[\text{Cu}_4\text{I}_4\text{C}_{38}\text{H}_{33}\text{N}_8]^+$: $m/z = 1362.6048$ (calad. 1362.6180).

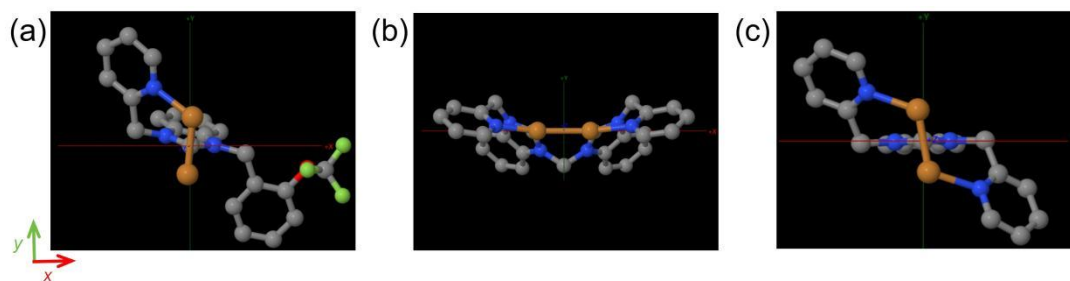


Figure S5. Cu_2 motifs in z -axis direction for (a) $\text{Cu}_2\text{NHC}^{\text{PyOF}}$ extracted from $\text{Cu}_2\text{I}_2(\text{NHC}^{\text{PyOF}})_2$; (b) $\text{Cu}_2\text{bisNHC}^{\text{Me}}$ extracted from $\text{Cu}_3\text{I}_3(\text{bisNHC}^{\text{Me}})$; and (c) $\text{Cu}_2\text{NHC}^{\text{Py}2}$ extracted from $\text{Cu}_4\text{I}_4(\text{NHC}^{\text{Py}2})_2$.

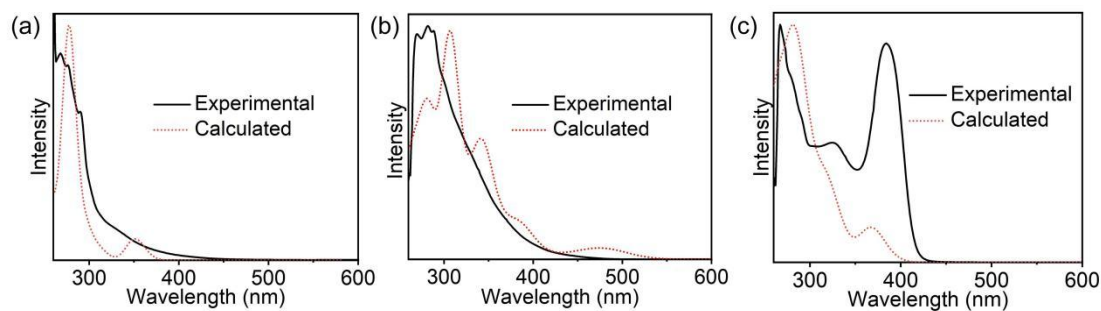


Figure S6. Experimental (black solid line) and calculated (red dotted line) UV-Vis absorption spectra of NHC-protected Cu(I) clusters of (a) $\text{Cu}_2\text{I}_2(\text{NHC}^{\text{PyOF}})_2$; (b) $\text{Cu}_3\text{I}_3(\text{bisNHC}^{\text{Me}})$; and (c) $\text{Cu}_4\text{I}_4(\text{NHC}^{\text{Py}_2})_2$.

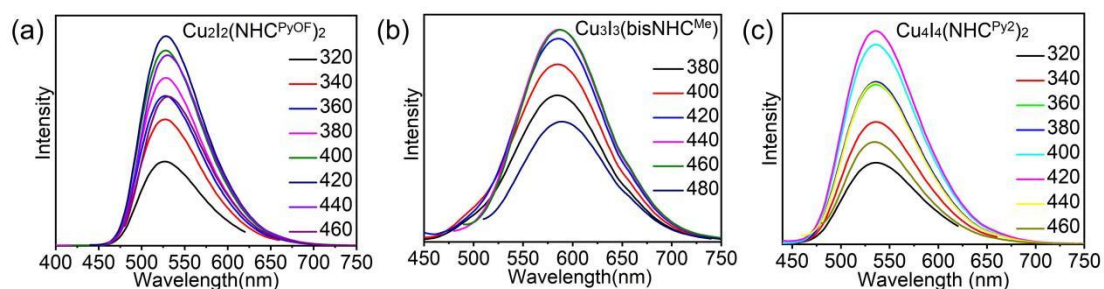


Figure S7. Emission spectra of (a) $\text{Cu}_2\text{I}_2(\text{NHC}^{\text{PyOF}})_2$; (b) $\text{Cu}_3\text{I}_3(\text{bisNHC}^{\text{Me}})$; and (c) $\text{Cu}_4\text{I}_4(\text{NHC}^{\text{Py}_2})_2$ excited at variable excitation wavelength in solid.

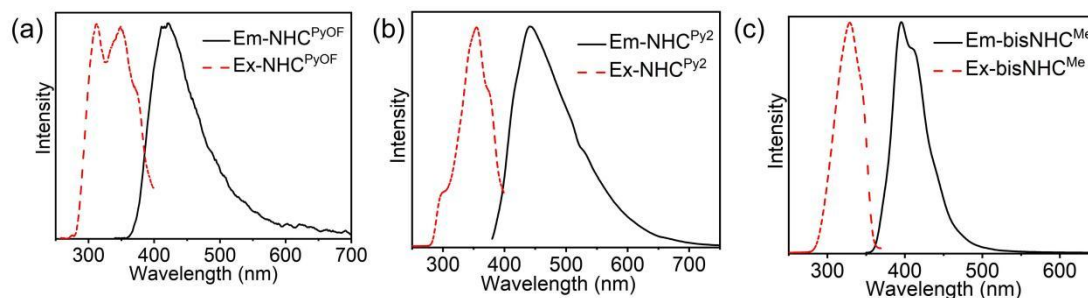


Figure S8. Emission (black solid line) and excitation spectra (red dotted line) of benzimidazole precursors (a) $\text{NHC}^{\text{PyOF}}\cdot\text{HCl}$; (b) $\text{bisNHC}^{\text{Me}}\cdot(\text{HCl})_2$; and (c) $\text{NHC}^{\text{Py}_2}\cdot\text{HCl}$ in *N,N*-dimethylformamide at room temperature. The sample concentrations were $\text{NHC}^{\text{PyOF}}\cdot\text{HCl}$ in 1.7×10^{-5} M, $\text{bisNHC}^{\text{Me}}\cdot(\text{HCl})_2$ in 2.9×10^{-5} M and $\text{NHC}^{\text{Py}_2}\cdot\text{HCl}$ in 3.3×10^{-5} M, respectively.

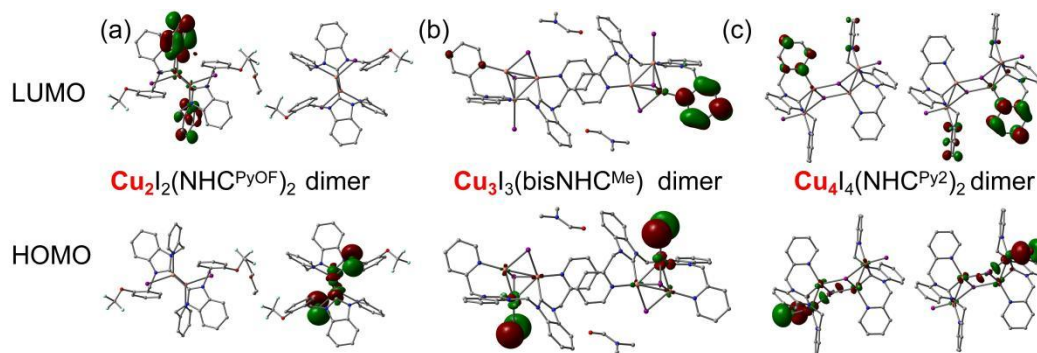


Figure S9. The frontier molecular orbitals (isovalue = 0.04) of dimer of NHC-protected Cu(I) clusters (a) $\text{Cu}_2\text{I}_2(\text{NHC}^{\text{PyOF}})_2$ dimer; (b) $\text{Cu}_3\text{I}_3(\text{bisNHC}^{\text{Me}})$ dimer; and (c) $\text{Cu}_4\text{I}_4(\text{NHC}^{\text{Py}2})_2$ dimer. The hydrogen atoms were hidden for the sake of viewing.

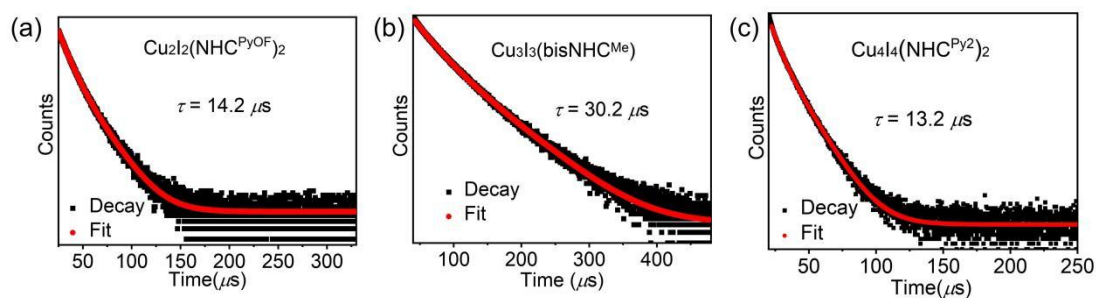


Figure S10. Lifetimes at room temperature for (a) $\text{Cu}_2\text{I}_2(\text{NHC}^{\text{PyOF}})_2$; (b) $\text{Cu}_3\text{I}_3(\text{bisNHC}^{\text{Me}})$; and (c) $\text{Cu}_4\text{I}_4(\text{NHC}^{\text{Py}2})_2$.

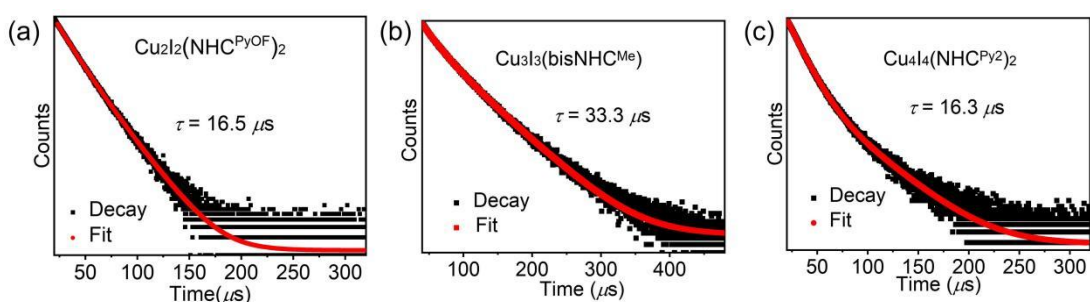


Figure S11. Lifetimes at 77 K for (a) $\text{Cu}_2\text{I}_2(\text{NHC}^{\text{PyOF}})_2$; (b) $\text{Cu}_3\text{I}_3(\text{bisNHC}^{\text{Me}})$; and (c) $\text{Cu}_4\text{I}_4(\text{NHC}^{\text{Py}2})_2$.

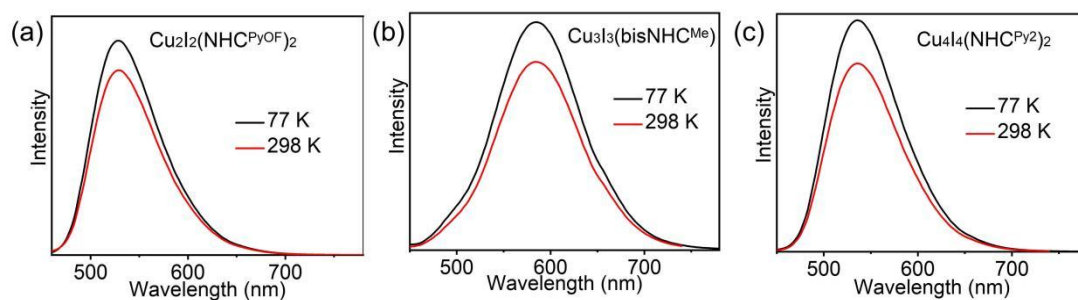


Figure S12. Emission spectra in solid at 77 K (black solid line) and 298 K (red solid line) for (a) $\text{Cu}_2\text{I}_2(\text{NHC}^{\text{PyOF}})_2$; (b) $\text{Cu}_3\text{I}_3(\text{bisNHC}^{\text{Me}})$; and (c) $\text{Cu}_4\text{I}_4(\text{NHC}^{\text{Py}_2})_2$.

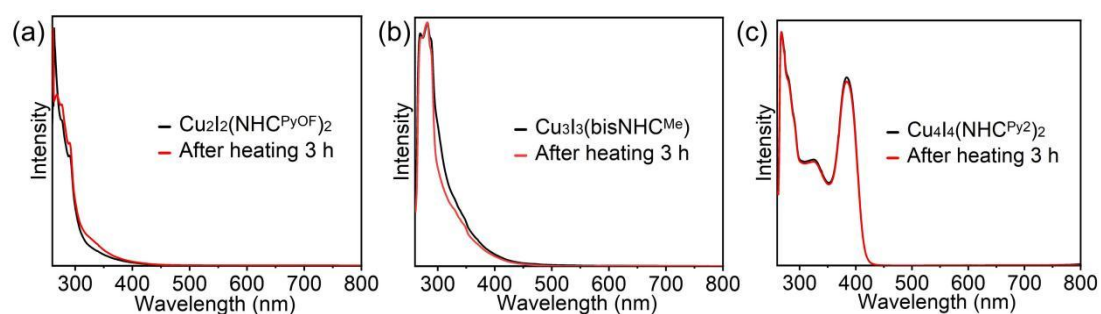


Figure S13. UV-Vis absorption spectra of the NHC-protected Cu(I) clusters in *N,N*-dimethylformamide before and after aging at 100 °C for 3 h: (a) $\text{Cu}_2\text{I}_2(\text{NHC}^{\text{PyOF}})_2$, 2.9×10^{-5} M; (b) $\text{Cu}_3\text{I}_3(\text{bisNHC}^{\text{Me}})$, 3.8×10^{-5} M; and (c) $\text{Cu}_4\text{I}_4(\text{NHC}^{\text{Py}_2})_2$, 4.5×10^{-5} M.

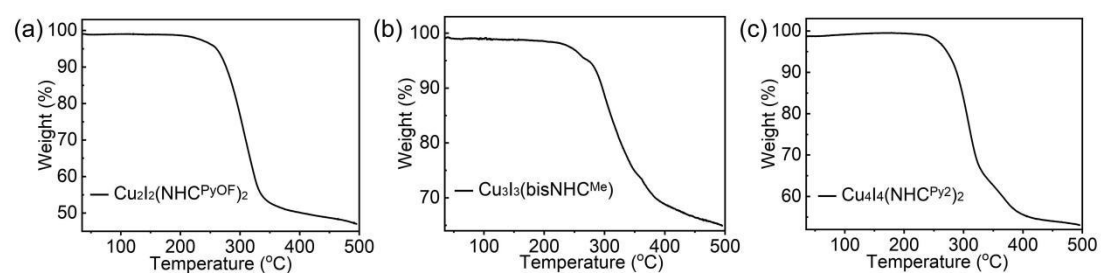


Figure S14. Thermogravimetric analysis (TGA) of (a) $\text{Cu}_2\text{I}_2(\text{NHC}^{\text{PyOF}})_2$; (b) $\text{Cu}_3\text{I}_3(\text{bisNHC}^{\text{Me}})$; and (c) $\text{Cu}_4\text{I}_4(\text{NHC}^{\text{Py}_2})_2$.

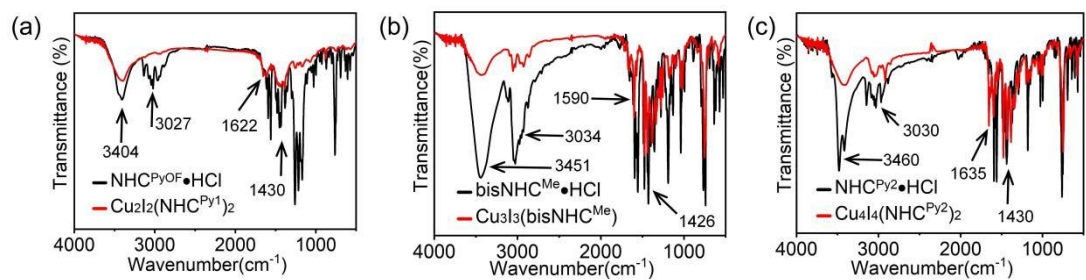


Figure S15. Fourier transform infrared spectroscopy (FTIR) of (a) $\text{Cu}_2\text{I}_2(\text{NHCPyOF})_2$; (b) $\text{Cu}_3\text{I}_3(\text{bisNHC}^{\text{Me}})$; and (c) $\text{Cu}_4\text{I}_4(\text{NHCPy}_2)_2$.

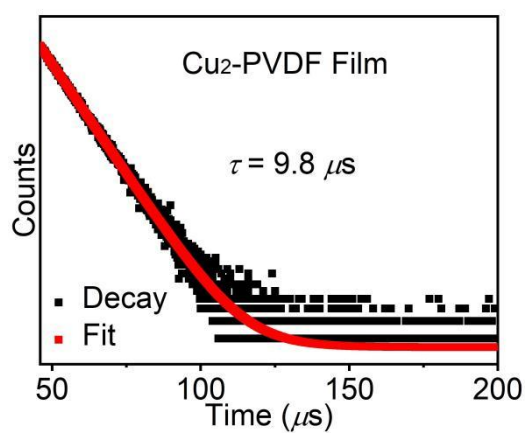


Figure S16. Lifetime for Cu_2 -PVDF film at room temperature.

Table S1. Major contributions of frontiers molecular orbitals for calculated UV-Vis spectrum of $\text{Cu}_2\text{I}_2(\text{NHC}^{\text{PyOF}})_2$.

Wavelength	Major Contributions
375 nm	<p>HOMO → LUMO (95%)</p>
330 nm	<p>HOMO → LUMO+2 (83%)</p>
291 nm	<p>HOMO-3 → LUMO (51%) HOMO-1 → LUMO+3 (33%)</p>
277 nm	<p>HOMO-4 → LUMO (51%) HOMO → LUMO+5 (23%)</p>
260 nm	<p>HOMO-3 → LUMO+2 (77%)</p>

Table S2. Major contributions of frontiers molecular orbitals for calculated UV-Vis spectrum of $\text{Cu}_3\text{I}_3(\text{bisNHC}^{\text{Me}})$.

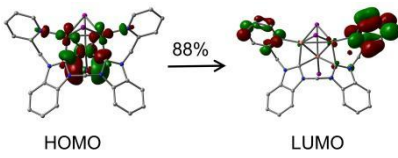
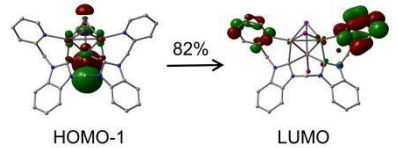
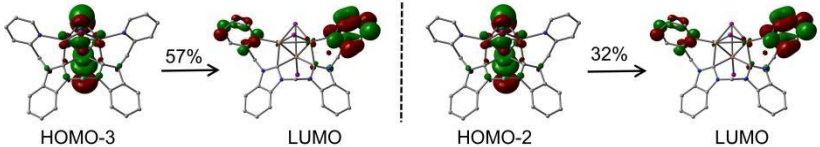
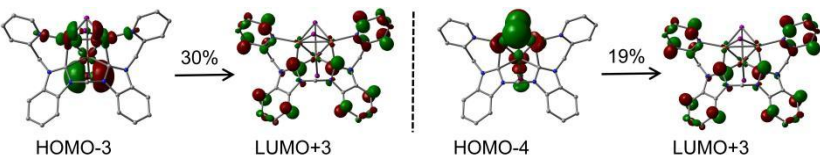
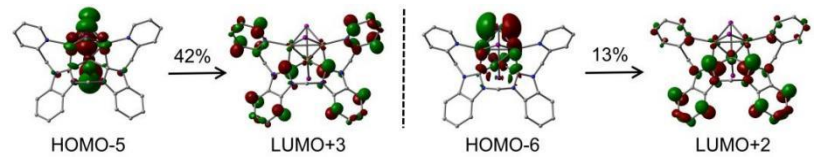
Wavelength	Major Contributions
450 nm	 <p>HOMO → LUMO (88%)</p>
383 nm	 <p>HOMO-1 → LUMO (82%)</p>
343 nm	 <p>HOMO-3 → LUMO (57%) HOMO-2 → LUMO (32%)</p>
308 nm	 <p>HOMO-3 → LUMO+3 (30%) HOMO-4 → LUMO+3 (19%)</p>
285 nm	 <p>HOMO-5 → LUMO+3 (42%) HOMO-6 → LUMO+2 (13%)</p>

Table S3. Major contributions of frontiers molecular orbitals for calculated UV-Vis spectrum of $\text{Cu}_4\text{I}_4(\text{NHC}^{\text{Py}^2})_2$.

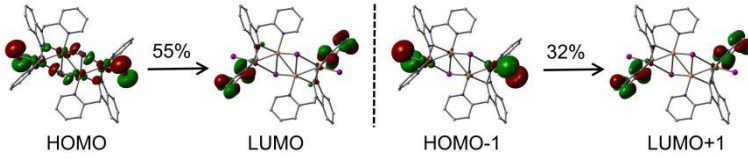
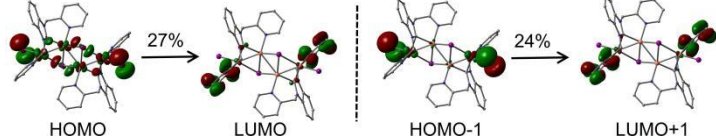
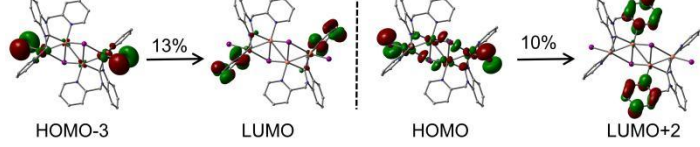
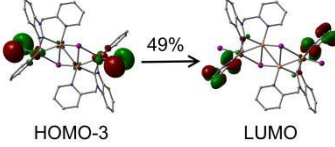
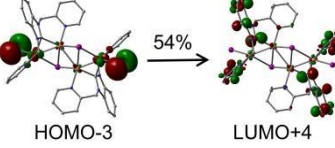
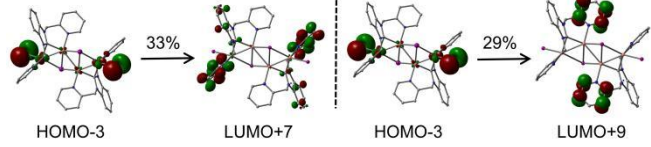
Wavelength	Major Contributions
413 nm	
366 nm	
	
338 nm	
296 nm	
270 nm	

Table S4. Crystal data and structure refinement for **Cu₂I₂(NHC^{PyOF})₂**.

Cu₂I₂(NHC^{PyOF})₂	
Empirical formula	C ₄₆ H ₄₂ Cu ₂ F ₆ I ₂ N ₆ O ₃
Formula weight	1221.73
Temperature/K	200.00(10)
Crystal system	triclinic
Space group	P-1
a/Å	10.2327(5)
b/Å	10.4416(5)
c/Å	24.6057(12)
α/°	91.419(4)
β/°	100.077(4)
γ/°	110.999(4)
Volume/Å ³	2405.6(2)
Z	2
ρ _{calc} /cm ³	1.687
μ/mm ⁻¹	11.759
F(000)	1204.0
Crystal size/mm ³	0.1 × 0.1 × 0.1
Radiation	Cu Kα (λ = 1.54184)
2θ range for data collection/°	7.332 to 130.168
Index ranges	-12 ≤ h ≤ 12, -12 ≤ k ≤ 7, -28 ≤ l ≤ 20
Reflections collected	12071
Independent reflections	6934 [R _{int} = 0.0610, R _{sigma} = 0.0832]
Data/restraints/parameters	6934/52/540
Goodness-of-fit on F ²	1.076
Final R indexes [I ≥ 2σ (I)]	R ₁ = 0.0865, wR ₂ = 0.2424
Final R indexes [all data]	R ₁ = 0.1138, wR ₂ = 0.2575
Largest diff. peak/hole / e Å ⁻³	2.38/-1.06
CCDC	2348356

Table S5. Selected bond lengths in $\text{Cu}_2\text{I}_2(\text{NHC}^{\text{PyOF}})_2$.

Atom	Atom	Length/Å	Atom	Atom	Length/Å
I1	Cu1	2.586(2)	C16	C18	1.39(2)
I2	Cu2	2.622(2)	F3	C17	1.30(3)
Cu1	Cu11	2.483(4)	O2	C43	1.405(19)
Cu1	N31	2.069(12)	O2	C11	1.417(14)
Cu1	C41	2.419(6)	C20	C28	1.529(13)
Cu1	C4	1.989(7)	C22	C38	1.523(18)
Cu2	Cu22	2.541(4)	C22	C40	1.39(2)
Cu2	C82	2.456(4)	C24	C40	1.37(2)
Cu2	C8	1.976(6)	C24	C44	1.36(3)
Cu2	N52	2.062(11)	C26	C28	1.39
N1	C8	1.366(6)	C26	C36	1.39
N1	C20	1.465(13)	C28	C30	1.39
N1	C13	1.363(2)	C30	C32	1.39
O1	C26	1.396(13)	C32	C34	1.39
O1	C17	1.35(2)	C34	C36	1.39
N4	C6	1.441(14)	F2	C17	1.38(3)
N4	C8	1.359(8)	C42	C44	1.37(2)
N4	C25	1.362(5)	C46	C23	1.39
N6	C4	1.349(9)	C46	C27	1.39
N6	C38	1.439(17)	C23	C3	1.39
N6	C7	1.375(9)	C3	C25	1.39
N3	C22	1.369(18)	C25	C13	1.39
N3	C42	1.333(17)	C13	C27	1.39
N2	C1	1.458(15)	C7	C29	1.39
N2	C4	1.338(15)	C7	C33	1.39
N2	C33	1.369(6)	C29	C15	1.39
O3	C19	1.385(14)	C15	C31	1.39
O3	C41	1.34(3)	C31	C2	1.39
F1	C41	1.30(3)	C2	C33	1.39
F4	C17	1.23(2)	F5	C41	1.32(3)
C1	C37	1.535(14)	C35	C9	1.39
F6	C41	1.33(3)	C35	C5	1.39
C6	C12	1.488(17)	C9	C37	1.39
C10	C12	1.402(19)	C37	C19	1.39
C10	C18	1.39(2)	C19	C39	1.39
C12	N5	1.340(16)	C39	C5	1.39
N5	C14	1.347(17)	C21	C43	1.527(10)
C14	C16	1.37(2)	C11	C45	1.530(10)

Table S6. Crystal data and structure refinement for **Cu₃I₃(bisNHC^{Me})**.

Cu₃I₃(bisNHC^{Me})	
Empirical formula	C ₃₁ H ₂₉ Cu ₃ I ₃ N ₆ O
Formula weight	1072.92
Temperature/K	200.00
Crystal system	triclinic
Space group	P-1
a/Å	8.3978(3)
b/Å	11.9863(5)
c/Å	18.0621(7)
α/°	74.184(4)
β/°	86.836(3)
γ/°	77.971(3)
Volume/Å ³	1710.86(12)
Z	2
ρ _{calc} /g/cm ³	2.083
μ/mm ⁻¹	23.691
F(000)	1022.0
Crystal size/mm ³	0.06 × 0.06 × 0.05
Radiation	Cu Kα (λ = 1.54184)
2θ range for data collection/°	7.826 to 147.164
Index ranges	-7 ≤ h ≤ 10, -14 ≤ k ≤ 14, -22 ≤ l ≤ 21
Reflections collected	16425
Independent reflections	6635 [R _{int} = 0.0639, R _{sigma} = 0.0693]
Data/restraints/parameters	6635/0/399
Goodness-of-fit on F ₂	1.096
Final R indexes [I ≥ 2σ (I)]	R ₁ = 0.0859, wR ₂ = 0.2474
Final R indexes [all data]	R ₁ = 0.0918, wR ₂ = 0.2514
Largest diff. peak/hole / e Å ⁻³	3.33/-2.26
CCDC	2269842

Table S7. Selected bond lengths in **Cu₃I₃(bisNHC^{Me})**.

Atom	Atom	Length/Å	Atom	Atom	Length/Å
I1	Cu3	2.664(2)	N6	C5	1.32(2)
I1	Cu2	2.839(2)	N6	C1	1.329(19)
I1	Cu1	2.723(2)	C5	C6	1.53(2)
I3	Cu3	2.548(2)	C5	C4	1.39(2)
I2	Cu2	2.617(2)	C13	C8	1.402(18)
I2	Cu1	2.576(2)	C13	C12	1.421(18)
Cu3	Cu2	2.577(3)	C8	C9	1.39(2)
Cu3	Cu1	2.519(3)	C9	C10	1.40(2)
Cu3	C15	1.966(13)	C10	C11	1.39(2)
Cu3	C7	2.317(12)	C11	C12	1.35(2)
Cu2	Cu1	2.605(3)	O1	C28	1.19(2)
Cu2	N6	2.066(12)	C21	C20	1.371(18)
Cu2	C7	1.978(13)	C21	C16	1.415(17)
Cu1	N5	2.025(11)	C20	C19	1.402(19)
Cu1	C15	2.369(13)	C19	C18	1.37(2)
N2	C13	1.379(17)	C18	C17	1.38(2)
N2	C14	1.484(16)	C17	C16	1.384(18)
N2	C7	1.364(16)	C29	C28	1.33(2)
N3	C16	1.384(16)	C29	C31	1.46(3)
N3	C14	1.463(15)	C29	C30	1.44(3)
N3	C15	1.365(15)	C22	C23	1.51(2)
N5	C23	1.357(19)	C1	C2	1.39(2)
N5	C27	1.30(2)	C4	C3	1.39(2)
N1	C8	1.395(17)	C23	C24	1.35(2)
N1	C6	1.469(16)	C26	C27	1.41(2)
N1	C7	1.331(17)	C26	C25	1.37(3)
N4	C21	1.397(16)	C2	C3	1.36(3)
N4	C22	1.457(15)	C24	C25	1.43(3)
N4	C15	1.364(17)			

Table S8. Crystal data and structure refinement for **Cu₄I₄(NHC^{Py2})₂**.

Cu₄I₄(NHC^{Py2})₂	
Empirical formula	C ₃₈ H ₃₂ Cu ₄ I ₄ N ₈
Formula weight	1362.47
Temperature/K	200.00
Crystal system	triclinic
Space group	<i>P</i> -1
<i>a</i> /Å	8.9031(4)
<i>b</i> /Å	11.2513(5)
<i>c</i> /Å	12.7832(6)
α /°	105.145(4)
β /°	100.155(4)
γ /°	100.596(4)
Volume/Å ³	1180.51(10)
<i>Z</i>	1
$\rho_{\text{calc}}/\text{cm}^3$	1.917
μ/mm^{-1}	22.829
<i>F</i> (000)	644.0
Crystal size/mm ³	0.03 × 0.02 × 0.02
Radiation	Cu K α (λ = 1.54184)
2 θ range for data collection/°	8.39 to 148.316
Index ranges	-10 ≤ <i>h</i> ≤ 11, -13 ≤ <i>k</i> ≤ 13, -15 ≤ <i>l</i> ≤ 10
Reflections collected	11573
Independent reflections	4558 [<i>R</i> _{int} = 0.0540, <i>R</i> _{sigma} = 0.0624]
Data/restraints/parameters	4558/92/244
Goodness-of-fit on <i>F</i> ₂	1.054
Final <i>R</i> indexes [<i>I</i> ≥ 2 σ (<i>I</i>)]	<i>R</i> ₁ = 0.0891, <i>wR</i> ₂ = 0.2563
Final <i>R</i> indexes [all data]	<i>R</i> ₁ = 0.1032, <i>wR</i> ₂ = 0.2679
Largest diff. peak/hole / e Å ⁻³	3.40/-2.86
CCDC	2270031

Table S9. Selected bond lengths in **Cu₄I₄(NHC^{Py2})₂**.

Atom	Atom	Length/Å	Atom	Atom	Length/Å
I2	Cu2	2.640(2)	N4	C15	1.392(9)
I2	Cu21	2.643(2)	C19	C18	1.389(10)
I2	Cu11	2.795(2)	C18	C17	1.389(10)
I1	Cu1	2.559(2)	C17	C16	1.382(10)
Cu2	Cu1	2.437(3)	C16	C15	1.382(9)
Cu2	N4	2.075(13)	C15	C14	1.49(2)
Cu2	C7	2.028(13)	C5	C6	1.51(2)
Cu1	N1	2.078(11)	C5	C4	1.38(2)
Cu1	C7	2.077(13)	C11	C10	1.391(9)
N3	C13	1.356(15)	C11	C12	1.391(9)
N3	C7	1.351(17)	C10	C9	1.390(9)
N3	C14	1.477(17)	C9	C8	1.386(9)
N2	C8	1.381(16)	C8	C13	1.390(9)
N2	C6	1.467(18)	C13	C12	1.382(9)
N2	C7	1.373(18)	C1	C2	1.383(10)
N1	C5	1.384(9)	C3	C4	1.40(3)
N1	C1	1.402(10)	C3	C2	1.37(3)
N4	C19	1.417(9)			

References

- (S1) X. Zhang, S. Gu, Q. Xia and W. Chen, New Structural Motifs of Silver and Gold Complexes of Pyridine-Functionalized Benzimidazolylidene Ligands. *J. Organomet. Chem.*, 2009, **694**, 2359-2367.
- (S2) M. C. Jahnke, T. Pape and F. E. Hahn, Synthesis and Catalytic Application of Palladium Complexes with Picoline-Functionalized Benzimidazolylidene Ligands. *Eur. J. Inorg. Chem.*, 2009, **2009**, 1960-1969.
- (S3) CrysAlis^{Pro} Version 1.171.36.31. 2012. Agilent Technologies Inc. Santa Clara, CA, USA.
- (S4) G. M. Sheldrick, A Short History of SHELX. *Acta Cryst., A* 2007, **64**, 112-122.
- (S5) O. V. Dolomanov, L. J. Bourhis, R. J. Gildea, J. A. K. Howard and H. Puschmann, OLEX2: A Complete Structure Solution, Refinement and Analysis Program. *J. Appl. Cryst.*, 2009, **42**, 339-341.
- (S6) G. M. Sheldrick, Crystal Structure Refinement with SHELXL. *Acta Cryst. C* 2015, **71**, 3-8.
- (S7) M. J. Frisch, G.W. Trucks and H.B. Schlegel, Gaussian 16 (Revision A.03). 2016.
- (S8) (a) W. Humphrey, A. Dalke and K. Schulten, VMD: Visual Molecular Dynamics. *J. Molec. Graphics*, 1996, **14**, 33-38. (b) J. P. Perdew, K. Burke and M. Ernzerhof, Generalized Gradient Approximation Made Simple. *Phys. Rev. Lett.*, 1996, **77**, 3865-3868. (c) G. A. Petersson, A. Bennett, T. G. Tensfeldt, M. A. Al-Laham, W. A. Shirley and J. Mantzaris, A Complete Basis Set Model Chemistry. I. The Total Energies of Closed-Shell Atoms and Hydrides of the First-Row Elements. *J. Chem. Phys.*, 1988, **89**, 2193-2218. (d) G. A. Petersson and M. A. Al-Laham, A Complete Basis Set Model Chemistry. II. Open-Shell Systems and the Total Energies of the First-Row Atoms. *J. Chem. Phys.*, 1991, **94**, 6081-6090. (e) P. Fuentealba, H. Preuss, H. Stoll and L. Von Szentpály, A Proper Account of Core-Polarization with Pseudopotentials: Single Valence-Electron Alkali Compounds. *Chem. Phys. Lett.*, 1982, **89**, 418-422.
- (S9) T. Lu and F. Chen, Multiwfn: A Multifunctional Wavefunction Analyzer. *J. Comput. Chem.*, 2012, **33**, 580-592.